

Model Independent Extraction of the Proton Charge Radius from PRad data

GIL PAZ

*Department of Physics and Astronomy
Wayne State University, Detroit, Michigan 48201, USA*

Abstract

The proton radius puzzle has motivated several new experiments that aim to extract the proton charge radius and resolve the puzzle. Recently PRad, a new electron-proton scattering experiment at Jefferson Lab, reported a proton charge radius of $0.831 \pm 0.007_{\text{statistical}} \pm 0.012_{\text{systematic}}$. The value was obtained by using a rational function model for the proton electric form factor. We perform a model-independent extraction using z -expansion of the proton charge radius from PRad data. We find that the model-independent statistical error is more than 50% larger compared to the statistical error reported by PRad.

1 Introduction

The proton is a composite particle. One way to define its size is by the proton charge radius, r_E^p . It is related to the slope of the proton electric form factor, G_E^p , at $q^2 = 0$, see (2) below. Since G_E^p is a non-perturbative function of q^2 , its slope must be extracted from data. The most direct way to measure r_E^p is by extracting G_E^p from lepton-proton scattering and finding its slope at $q^2 = 0$. An indirect way is by using atomic spectroscopy.

Thus we have four different methods to extract r_E^p from data: $e - p$ scattering, $\mu - p$ scattering, $e - p$ spectroscopy, and $\mu - p$ spectroscopy. A fifth method, Lattice QCD, should become competitive in the future, see, e.g., [1]. While $e - p$ scattering and spectroscopy extractions were available for a long time, $\mu - p$ spectroscopy only became available in 2010 from the work of the CREMA collaboration [2, 3]. Results from $\mu - p$ scattering are expected in the near future from the MUSE collaboration [4]. Ideally, all methods should give consistent results. Surprisingly, in 2010, $\mu - p$ spectroscopy gave a value, 0.84184(67) fm, that was considerably smaller than the CODATA value, 0.8768(69) fm [5]. This difference is referred to as the “proton radius puzzle”. For a recent review, see [6].

The puzzle has motivated new theoretical and experimental work. Three new $e - p$ spectroscopy measurements were published recently. Two agree with the smaller value [7, 8], and one [9] with the larger value. Two new $e - p$ scattering experiments, ISR and PRad, have published their results and more experiments are planned [10]. ISR found 0.81(8) fm [11] which cannot distinguish between the two values. PRad found [12] $0.831 \pm 0.007_{\text{statistical}} \pm 0.012_{\text{systematic}}$ fm, which favors the smaller value.

A main issue in extracting r_E^p from scattering data is the assumed functional form of G_E^p . Recent extractions have used: dipole [13], polynomial [14, 15], continued fraction [14], modified z expansion [16], or more complicated forms [17]. For pre-2010 extractions see [18]. Different functional forms can lead to *different* radii and uncertainties from the *same* data. An alternative approach is the so-called z expansion that only uses the known analytic structure of G_E^p . The z expansion is the default method for meson form factors. It was first applied to baryon form factors in [19]. Extractions of r_E^p using z expansion favor the larger value [19, 20].

The default functional form for G_E^p used by PRad is a rational function called “Rational (1,1)”, see (5) below. Apart from the overall normalization (that does not affect the slope) it depends on two parameters. In [19] it was shown that a fit with a small number of parameters can underestimate the errors. In figure S15 of the supplementary material of the PRad paper [12], the “Rational (1,1)” fit and “2nd order z -tran.” give similar radii with similar uncertainty, but “3rd order z -tran.” has twice the uncertainty. As was shown in [19], adding higher powers of z without bounding the coefficients will cause the uncertainty to grow without bound. On the other hand, If we bound the coefficients, we obtain an extraction of r_E^p that is independent of the number of the parameters we fit [19]. Since the form factor must have the correct analytic structure and therefore can be expanded as Taylor series in z , we obtain an extraction of r_E^p that is independent of the exact unknown functional form of the form factor.

The goal of this paper is to perform such a model-independent analysis to the published PRad data and to see how it affects the errors on the extracted r_E^p . For simplicity, we use

the values of G_E^p reported by PRad in [21] and use only the statistical errors¹. The rest of the paper is organized as follows. In section 2 we briefly review the relevant form factor parameterization and the z expansion. In section 3 we repeat the fits performed by PRad to its data and reproduce their results. In section 4 we perform a model-independent z -expansion fit to the PRad data and extract r_E^p . We present our conclusions in section 5.

2 Form factor parameterization and the z expansion

The one-photon probe of the proton gives rise to two form factors, F_1^p and F_2^p ,

$$\langle P(p') | J_\mu^{\text{em}} | P(p) \rangle = \bar{u}(p') \left[\gamma_\mu F_1^p(q^2) + \frac{i\sigma_{\mu\nu}}{2m_p} F_2^p(q^2) q^\nu \right] u(p), \quad (1)$$

where $q^2 = (p' - p)^2 \equiv t \equiv -Q^2$. The electric and magnetic form factors are defined as [22] $G_E^p(q^2) = F_1^p(q^2) + q^2 F_2^p(q^2)/4m_p^2$ and $G_M^p(q^2) = F_1^p(q^2) + F_2^p(q^2)$. The proton charge radius squared is defined via the slope of $G_E^p(q^2)$ at $q^2 = 0$:

$$\langle r^2 \rangle_E^p = \frac{6}{G_E^p(0)} \left. \frac{d}{dq^2} G_E^p(q^2) \right|_{q^2=0}. \quad (2)$$

The proton charge radius is given by $r_E^p \equiv \sqrt{\langle r^2 \rangle_E^p}$. In [12] r_E^p is denoted by r_p .

$G_E^p(q^2)$ is analytic in the complex q^2 plane outside a cut that starts at the two-pion threshold $q^2 = 4m_\pi^2$. The domain of analyticity can be mapped onto the unit $|z| < 1$ circle via the transformation

$$z(t, t_{\text{cut}}, t_0) = \frac{\sqrt{t_{\text{cut}} - t} - \sqrt{t_{\text{cut}} - t_0}}{\sqrt{t_{\text{cut}} - t} + \sqrt{t_{\text{cut}} - t_0}}, \quad (3)$$

where $t_{\text{cut}} = 4m_\pi^2$ and t_0 determines the location of $z = 0$. In the following we use $t_0 = 0$. In the $|z| < 1$ unit circle G_E^p is analytic and can be expanded as a Taylor series:

$$G_E^p(q^2) = \sum_{k=0}^{\infty} a_k z(q^2)^k. \quad (4)$$

The choice $t_0 = 0$ implies that r_E^p depends only on a_1 .

Plotting the data as function of z can be very instructive. For example, when only a slope can be constrained, the z -dependent data will appear linear, while the Q^2 -dependent data can appear to have curvature. See, e.g., figure 3 in [23] for a mesonic form factor and figure 2 in [24] for a baryonic form factor. In figure 1 we plot G_E^p from the full PRad data set (described in the next section) as a function of Q^2 (left) and z (right). We can see a certain amount of curvature in the plot of G_E^p as a function of z . We will explore this further in section 4.3.

The default fit function used by PRad is

$$f(Q^2) = n G_E^p(Q^2) = n \frac{1 + p_1 Q^2}{1 + p_2 Q^2}. \quad (5)$$

¹Determining the systematic error for the charge radius is much more involved and described in the supplementary material of the PRad paper [12].

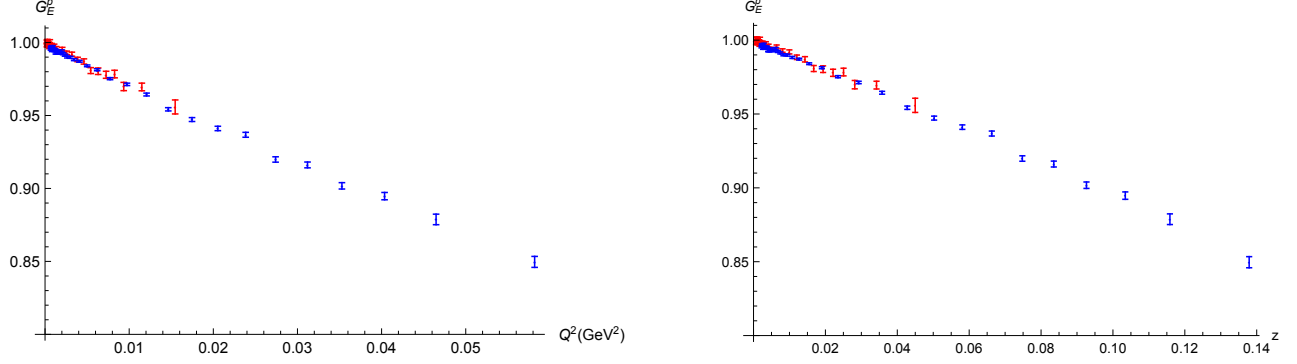


Figure 1: A comparison of G_E^p from the PRad data set as a function of Q^2 (left) and z (right). The 1.1 GeV (2.2 GeV) data set is in red (blue), the same color scheme used in [12].

In [12] it is referred to as “Rational (1,1)”. This function can be written as a sum of pole and a constant:

$$f(Q^2) = n \frac{1 + p_1 Q^2}{1 + p_2 Q^2} = n \frac{1 - p_1 t}{1 - p_2 t} = \frac{n(p_1 - p_2)/p_2^2}{t - 1/p_2} + \frac{np_1}{p_2}. \quad (6)$$

Provided that $1/p_2 > 4m_\pi^2$, this function’s singularity lies above the two-pion threshold. In order to have the correct analytic structure, we must have $1/p_2 > 4m_\pi^2$. We will check this requirement against PRad data in section 3.1.

Assuming $1/p_2 > 4m_\pi^2$, the Rational (1,1) function can be expressed as a Taylor series in z . The coefficients a_k depend on its imaginary part. Since this is a sum of pole and a constant, the imaginary part is a delta function. Using the expressions in [19] we find

$$\begin{aligned} a_0 &= f(0) \stackrel{\text{Rational (1,1)}}{=} n \\ a_{k \geq 1} &= \frac{2}{\pi} \int_{t_{\text{cut}}}^{\infty} \frac{dt}{t - t_0} \sqrt{\frac{t_{\text{cut}} - t_0}{t - t_{\text{cut}}}} \text{Im} f(t) \sin[k\theta(t)] \stackrel{\text{Rational (1,1)}}{=} \\ &= \frac{2n(p_1 - p_2)}{p_2} \sqrt{\frac{4m_\pi^2}{p_2^{-1} - 4m_\pi^2}} \sin \left[k \cos^{-1} \left(1 - 8p_2 m_\pi^2 \right) \right]. \end{aligned} \quad (7)$$

We will compare these expressions to a z -expansion fit to the PRad data in section 4.3.

3 PRad extractions of the proton charge radius

Before improving on the r_E^p extraction from the PRad data, we should reproduce its published results. We use the information in [12] and its supplementary material. We use the PRad data release [21] from December 10, 2019. The “raw” values of $G_E^p(Q^2)$ can be obtained from the “1.1GeV_table.txt” and “2.2GeV_table.txt” files, where they are listed under “f(Q2)”. The two files correspond to the 1.1-GeV and 2.2-GeV electron beams data of the PRad experiment.

We repeat many of the fits reported in [12] and its supplementary material. We focus on the default PRad Rational (1,1) fit and the fits involving the z expansion. We use the χ^2 function

$$\chi^2_{\text{PRad}} = \sum_{i=1}^N \frac{(G_{E,\text{exp}}^{p,i} - G_{E,\text{theo}}^{p,i})^2}{(\delta G_{E,\text{exp}}^{p,i})^2}, \quad (8)$$

And minimize it for a given theoretical expression of G_E^p . We use only the statistical errors in $\delta G_{E,\text{exp}}^{p,i}$. The proton charge radius is calculated via (2). The uncertainty is found by the $\delta\chi^2 = 1$ range. In reproducing the PRad fits we follow its practice and include a normalization factor for the data as a multiplicative factor in $G_{E,\text{theo}}^{p,i}$. This normalization factor is also determined from the fit.

3.1 Default PRad fit

The default expression for G_E^p used by PRad is the Rational (1,1) function given in (5). The Rational (1,1) is fitted to both the 1.1 GeV and 2.2 GeV with different overall normalization factors called n_1 and n_2 , but with the same p_1 and p_2 .

From our fit we find $n_1 = 1.0002 \pm 0.0002_{\text{statistical}}$, $n_2 = 0.9983 \pm 0.0002_{\text{statistical}}$, and $r_E^p = 0.831 \pm 0.007_{\text{statistical}}$ fm. The reduced χ^2 is 1.3. These are also the results in [12].

As a further check, we find that the fit values of p_1 and p_2 are $p_1 = -0.0715 \text{ GeV}^{-2}$ and $p_2 = 2.88 \text{ GeV}^{-2}$. Up to the first three significant figures, these are the values reported in “readme.pdf” in [21]. Including the uncertainties on these parameters, we find $p_1 = -0.07_{-0.54}^{+0.56} \text{ GeV}^{-2}$ and $p_2 = 2.88_{-0.59}^{+0.61} \text{ GeV}^{-2}$. Within the one standard deviation range we have $1/p_2 > 4m_\pi^2 \approx 0.0784 \text{ GeV}^2$. Thus the fit result is consistent with the analytic structure of G_E^p .

3.2 Other PRad fits

In the supplementary material of [12] the results of other fits to the PRad data are shown, but only in figures. Still, the approximate value of r_E^p and its statistical uncertainty can be inferred from the figures.

PRad performed fits to its entire data set using a second order and third order polynomial in z . These correspond to truncating the series in (4) at z^2 and z^3 , respectively. For example, equation (2) of the supplementary material is $f(Q^2) = nG_E^p(Q^2) = n(1 + p_1z + p_2z^2)$. Using these expressions with different normalizations for the 1.1 GeV and 2.2 GeV data, our fit to the PRad data gives $r_E^p = 0.830 \pm 0.008_{\text{statistical}}$ fm for the second order polynomial in z and $r_E^p = 0.825 \pm 0.015_{\text{statistical}}$ fm for the third order polynomial in z . These results agree with the values and statistical uncertainty in figure S15 of the supplementary material of [12]. Notice also that the uncertainty is doubled when changing from a second to a third order polynomial. We will address this problem below.

PRad also performed fits using Rational (1,1) to parts of the data set. These are listed in figure S16(a) of the supplementary material of [12]. Following PRad, we fitted the 1.1 GeV data, 2.2 GeV data, $Q^2 < 0.016 \text{ GeV}^2$ data, and $Q^2 > 0.002 \text{ GeV}^2$ data. We find $r_E^p = 0.845_{-0.039}^{+0.041}$ fm for the 1.1 GeV data only, $r_E^p = 0.829_{-0.008}^{+0.008}$ fm for the 2.2 GeV data only,

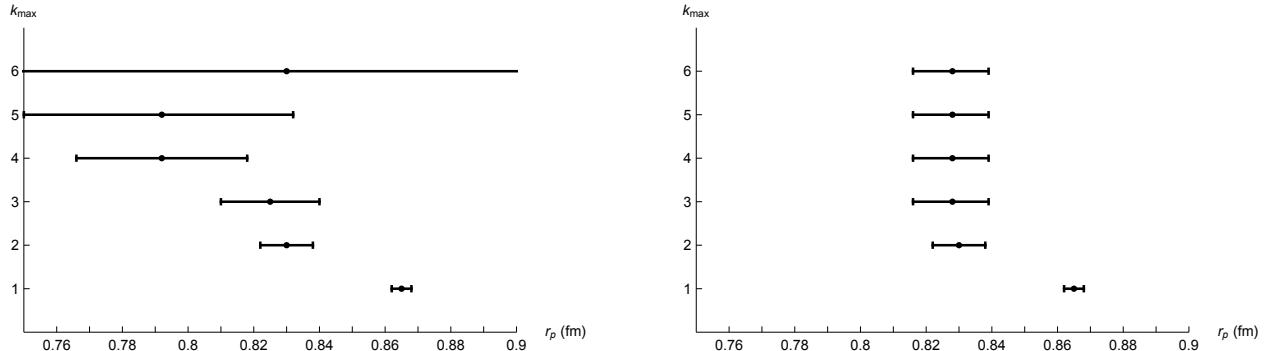


Figure 2: A comparison of the extracted r_E^p as a function of the number of fitted p_k parameters from z -expansion fits to the PRad data set. The range on the x -axis is the same range used in figure S15 of the supplementary material of [12]. Left: a fit without a bound on the coefficients p_k . Starting at $k_{\max} = 5$ the uncertainty on r_E^p exceeds the range 0.75 – 0.9 fm. Right: a fit with a bound of 5 on the coefficients p_k .

$r_E^p = 0.799^{+0.018}_{-0.017}$ fm for the $Q^2 < 0.016$ GeV² data, and $r_E^p = 0.841^{+0.011}_{-0.011}$ fm for the $Q^2 > 0.002$ GeV² data. All uncertainties are statistical. These results agree with figure S16(a).

Finally, PRad considered a fit of second order polynomial in z to the 2.2 GeV data only. Performing such a fit we find $r_E^p = 0.829 \pm 0.009_{\text{statistical}}$ fm. These results agree with figure S16(b) of the supplementary material of [12].

In conclusion, we reproduced the values of r_E^p reported by PRad from the PRad data. We now investigate if and how these results change when we use a model-independent extraction.

3.3 The need for a bound on the coefficients

Truncating the z -expansion series, as was done in the PRad fits, might underestimate the uncertainty of r_E^p . On the other hand, simply increasing the number of fitted parameters can overestimate the uncertainty. As shown in [19], one needs to bound the coefficients.

To illustrate that, we perform a fit to the PRad data of the form $f(Q^2) = nG_E^p(Q^2) = n(1 + p_1z + p_2z^2 + \dots + p_{k_{\max}}z^{k_{\max}})$. As in the PRad fits we use different normalization factors n_1 and n_2 for the 1.1 GeV and the 2.2 GeV data, but the same p_k for both data sets. We consider two cases, no bound on p_k and a bound $|p_k| < 5$. We implement the bound as in [20] by adding $\chi_{\text{Bound}}^2 = \sum_{k=0}^{k_{\max}} p_k^2/5^2$ to (9).

The results of the two fits are shown in figure 2 as a function of the number of fitted p_k parameters. As expected [19], the extracted value of r_E^p grows without bound for the unbounded fit, while for the bounded fit it stabilizes on $r_E^p = 0.828^{+0.011}_{-0.012}$ fm.

4 Model independent extraction of the proton charge radius

Below we perform a model-independent z -expansion fit to PRad data, that includes a bound on the coefficients. We consider a fit to the whole PRad data set as well as the 1.1 GeV and 2.2 GeV data subsets. We also explore the effects of the bound on the coefficients, the Q^2 dependence of the extracted r_E^p , and the possible extraction of a_k parameters beyond a_1 .

4.1 Model-independent z -expansion r_E^p extraction from the entire PRad data

We extract r_E^p from the PRad data by using the χ^2 function

$$\chi_z^2 = \sum_{i=1}^N \frac{(\eta_i G_{E, \text{exp.}}^{p,i} - G_{E, \text{theo.}}^{p,i})^2}{(\delta G_{E, \text{exp.}}^{p,i})^2}. \quad (9)$$

As before, $G_{E, \text{exp.}}^{p,i}$ are the values of G_E^p reported by PRad and $\delta G_{E, \text{exp.}}^{p,i}$ its statistical errors. $G_{E, \text{theo.}}^{p,i}$ is given in (4) where the series is truncated at k_{max} . The normalization factors are $\eta_i = \eta_1$ if i is part of the 1.1 GeV data set, and $\eta_i = \eta_2$ if i is part of the 2.2 GeV data set. Thus we allow for a normalization factor for each data set, but unlike PRad fits, we do not include it in $G_{E, \text{theo.}}^{p,i}$. Since we include a normalization factor, we fix $G_E^p(0) = 1$ which implies $a_0 = 1$ in the fits.

In order to bound the coefficients we add to χ_z^2 , as in [20], χ_{Bound}^2 defined as

$$\chi_{\text{Bound}}^2 = \sum_{k=0}^{k_{\text{max}}} \frac{a_k^2}{B^2}, \quad (10)$$

where B is a pure number. Our default value is $B = 5$, but we check our results also for $B = 10$.

Fitting the entire PRad data with $B = 5$, we find that the extracted proton charge radius is $r_E^p = 0.828_{-0.012}^{+0.011}$ fm. Changing the bound to $B = 10$ we find $r_E^p = 0.827_{-0.014}^{+0.013}$ fm. These are almost identical one-standard deviation ranges. Compared to the default PRad fit of Rational (1,1), $r_E^{p, \text{rational}} = 0.831 \pm 0.007$ fm, the central values are almost the same, but the uncertainty is more than 50% larger for the z -expansion fit. The extracted r_E^p stabilizes for $k_{\text{max}} = 3$. It does not change as we increase k_{max} above 3. We checked this with fits up to $k_{\text{max}} = 10$.

As another check, we consider fits without adding χ_{Bound}^2 and by using explicit bounds of $|a_k| \leq 5$ and $|a_k| \leq 10$ as in [19, 24]. We find $r_E^p = 0.824_{-0.012}^{+0.015}$ fm for $|a_k| \leq 5$ and $r_E^p = 0.824_{-0.015}^{+0.015}$ fm for $|a_k| \leq 10$. These are very close to the results above that used χ_{Bound}^2 .

4.2 Model-independent z -expansion r_E^p extraction from parts of the PRad data

The Rational (1,1) fits to the 1.1 GeV and 2.2 GeV parts of the PRad data give values of r_E^p that are within the one-standard deviation range of each other, but the uncertainty on the

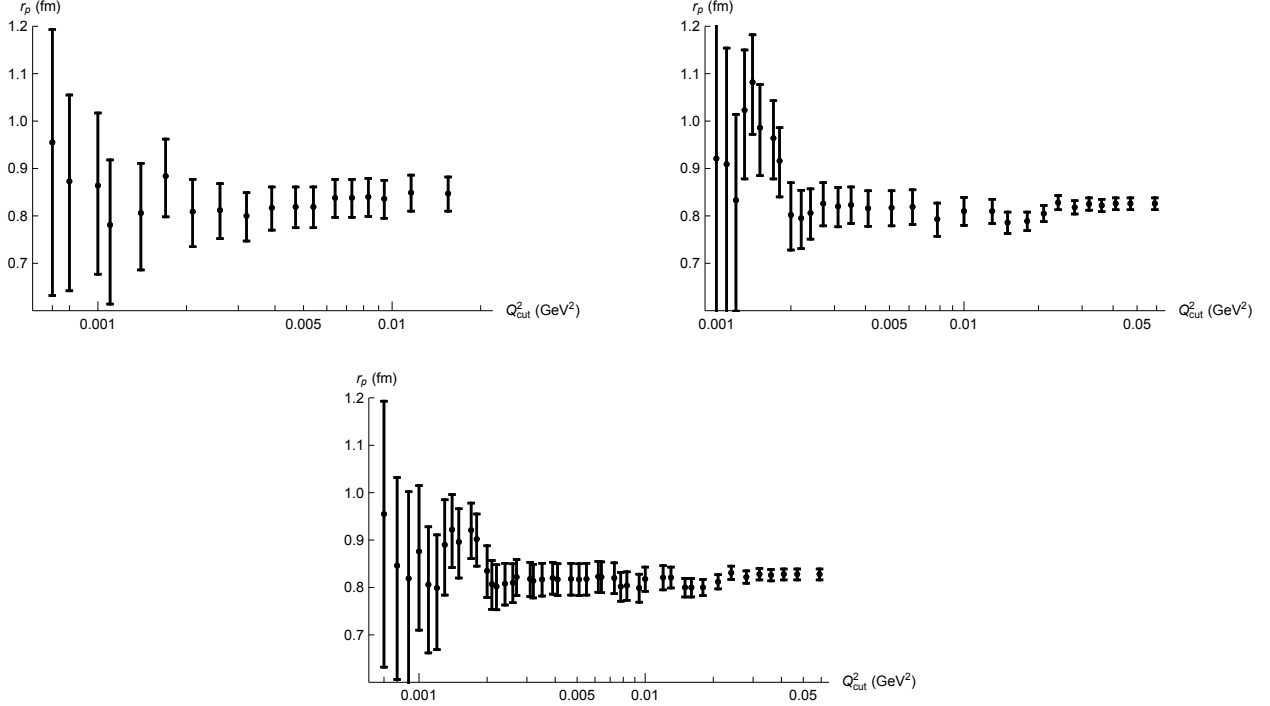


Figure 3: Extracted r_E^p as a function of Q_{cut}^2 . Top left: 1.1 GeV data set. Top right: 2.2 GeV data set. Bottom center: 1.1 and 2.2 GeV data sets.

former is five times as large. It is instructive to see what are the results for z -expansion fit. We use the same fit χ^2 function, namely the sum of χ_z^2 and χ_{Bound}^2 .

Using only the 1.1 GeV data set we find $r_E^p = 0.847_{-0.037}^{+0.035}$ fm for $B = 5$ and $r_E^p = 0.846_{-0.041}^{+0.039}$ fm for $B = 10$. These are almost identical to the Rational (1,1) fit result of $r_E^{p,\text{rational}} = 0.845_{-0.039}^{+0.041}$ fm. Using only the 2.2 GeV data set we find $r_E^p = 0.826_{-0.013}^{+0.012}$ fm for $B = 5$ and $r_E^p = 0.823_{-0.015}^{+0.015}$ fm for $B = 10$. These are consistent with the Rational (1,1) fit result of $r_E^{p,\text{rational}} = 0.829_{-0.008}^{+0.008}$ fm, but the uncertainty is more than 50% larger for the z -expansion fit.

Another question we study is the effect of a cut on Q^2 . We consider this question for the 1.1 GeV data alone, the 2.2 GeV data alone, and the combined 1.1 GeV and 2.2 GeV data. We perform fits to r_E^p for data with Q^2 smaller than Q_{cut}^2 . The lowest Q_{cut}^2 is determined by the requirement that the slope of the form factor is positive. If Q^2 is too small, we do not have enough data for a meaningful extraction of r_E^p . Thus $Q_{\text{cut}}^2 \in [0.0007, 0.0155]$ GeV² for the 1.1 GeV data set, $Q_{\text{cut}}^2 \in [0.001, 0.059]$ GeV² for the 2.2 GeV data set, and $Q_{\text{cut}}^2 \in [0.0007, 0.059]$ GeV² for the combined 1.1 GeV and 2.2 GeV data sets. All fits are performed with $B = 5$.

The results of the extractions are shown in figure 3. In all three plots we see a convergence to a value as Q_{cut}^2 is increased. In the 2.2 GeV data set plot and the combined 1.1 GeV and 2.2 GeV data sets we see also a “peak” at about $Q_{\text{cut}}^2 = 0.0014$ GeV². But overall the extraction is independent of the cut on Q^2 , for large enough Q_{cut}^2 .

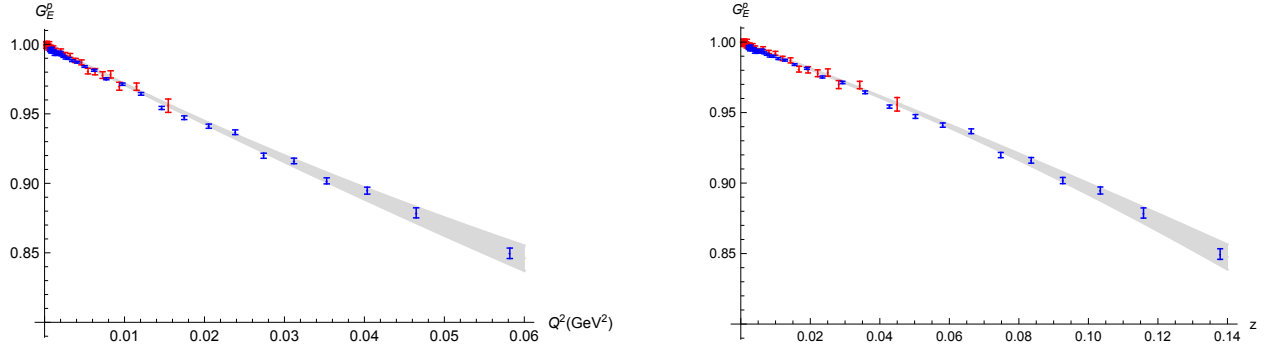


Figure 4: A model-independent z -expansion fit to G_E^p from the entire PRad data set (gray band) together with values of G_E^p from the PRad data set as a function of Q^2 (left) and z (right). The 1.1 GeV (2.2 GeV) data set is in red (blue), the same color scheme used in [12].

4.3 Model-independent z -expansion fit to the entire PRad data

The charge radius is only a one-parameter characterization of the data. We can try and extract more coefficients in (4). To do that we use (9) and add to it a modified version of (10) where we omit the term a_i^2/B^2 in the sum in (10) when constraining the a_i coefficient.

We perform such a fit to the full PRad data set (both 1.1 and 2.2 GeV) using $B = 5$. The fit stabilizes quickly for $k_{\max} = i + 3$. We find that $a_1 = -0.921 \pm 0.026$, $a_2 = -1.2 \pm 0.6$, and $a_3 = 2.2 \pm 5.7$. Using $B = 10$ gives very similar results. This implies that beyond a slope (a_1), only a curvature (a_2) can be obtained from the PRad data².

To compare these results graphically to the PRad data, we perform a fit with $B = 5$ to the full PRad data set without bounding a_1 and a_2 , i.e., we omit the terms a_1^2/B^2 and a_2^2/B^2 in the sum in (10). The fit stabilizes quickly with increasing k_{\max} . We find the values above for a_1 and a_2 and a covariance of -0.0137 between them. The variance of the data normalization factors $\eta_{1,2}$ is negligible as well as their covariance with a_1 or a_2 . The resulting fit and uncertainty [25] is shown in figure 4 together with the PRad data from figure 1.

5 Conclusions

The proton radius puzzle has motivated new theoretical and experimental work. Among them is PRad, a new electron-proton scattering experiment at Jefferson Lab. PRad reached the lowest Q^2 in $e - p$ scattering: $2.1 \times 10^{-4} \text{ GeV}^2$, an order of magnitude lower than previously achieved at A1 Mainz [26, 27]. The small Q^2 should allow to reduce extrapolation errors in extracting the proton charge radius.

PRad has extracted a radius of $0.831 \pm 0.007_{\text{statistical}} \pm 0.012_{\text{systematic}}$ fm by using a Rational (1,1) fit function for G_E^p . Instead of relying on a specific model for G_E^p , one can use a model-

²We can compare these values to the values predicted by the Rational (1,1) fit from section 3.1. Using $p_1 = -0.07_{-0.54}^{+0.56} \text{ GeV}^{-2}$ and $p_2 = 2.88_{-0.59}^{+0.61} \text{ GeV}^{-2}$, equation (7) gives $a_1^{\text{Rational (1,1)}} = -0.93 \pm 0.26$ and $a_2^{\text{Rational (1,1)}} = -1.02 \pm 0.19$. These agree with the values we obtained from the z -expansion fit

independent approach via the z expansion. In this paper we have examined how the statistical error reported by PRad changes when using such a model-independent approach.

In section 3 we repeated many of the fits performed by PRad to its data. These include its default Rational (1,1) fit to the entire PRad data, a second and third order polynomial in z fit to the entire PRad data, Rational (1,1) fit to parts of its data set, and a second order polynomial in z fit to its 2.2 GeV data. These agree with [12], its supplementary material, and information from the PRad data release [21] from December 10, 2019.

We also compared the extractions of r_E^p when higher polynomials in z are considered, with and without bounding the coefficients of the polynomial in z . The results appear in figure 2. As expected [19], we find that the extracted proton charge radius grows without bound for the unbounded fit, while for the bounded fit it stabilizes very quickly to a value independent of the degree of the z polynomial.

In section 4 we performed a model-independent z -expansion fit to PRad data. The bounding of the coefficients is implemented by adding a term to χ^2 [20], see (10). From a fit to the entire PRad data set we find $r_E^p = 0.828_{-0.012}^{+0.011}$ fm. Compared to the default PRad fit, $r_E^{p,\text{rational}} = 0.831 \pm 0.007$ fm, the central values are almost the same, but the uncertainty is more than 50% larger for the z -expansion fit. This implies that PRad's default fit underestimates the statistical error by using the Rational (1,1) function.

We also performed a model-independent z -expansion fit to parts of the PRad data. We fitted the 1.1 GeV and 2.2 GeV parts of the PRad data separately. For the 1.1 GeV data (that contains the smaller Q^2 data) we find that the model independent extraction is almost identical to the Rational (1,1) fit. The error bar of this extraction is too large to distinguish between the two values of the proton charge radius. For the 2.2 GeV data the model independent extraction uncertainty is 50% larger than the Rational (1,1) fit. We considered also the effects of a Q^2 cut on the data, $Q^2 < Q_{\text{cut}}^2$. The results are shown in figure 3 for the 1.1 GeV data, the 2.2 GeV data, and the entire PRad data. Overall the extraction is independent of the cut on Q^2 , for a large enough Q_{cut}^2 .

Going beyond r_E^p , we fitted more parameters in the z expansion to the PRad data. The results are described in section 4.3 and figure 4. We find that beyond the slope, equivalent to r_E^p , only a curvature can be obtained from the PRad data.

Before concluding, let us briefly review recent papers that also analyzed the PRad data. In [28] PRad data was analyzed to investigate its consistency with r_E^p from muonic hydrogen and theoretical predictions for the coefficients of Q^4 and Q^6 terms in the Q^2 expansion of G_E^p . Using a rational function to incorporate these inputs, the author of [28] found very good agreement with the PRad data. In [29] a fit using the DI χ EFT model to the PRad and A1 Mainz data [26, 27] was performed. The authors of [29] found the same value of r_E^p within uncertainties as their fit to A1 Mainz data alone. Finally, very recently [30] appeared that compared fits using the z -expansion to non-PRad scattering data and PRad data. The authors of [30] remark that their z -expansion fit to PRad data, taking the PRad errors at face value, results in a significantly larger uncertainty for r_E^p compared to the Rational (1,1) PRad fit.

In summary, using model-independent methods we find that the statistical uncertainty on the proton charge radius from the PRad data is more than 50% larger than the one quoted by PRad in [12]. The systematic error is obtained by a much more involved process that is described in the supplementary material of the PRad paper [12]. It is likely that the

systematic error will also increase when using model-independent methods. It is needed for a full model-independent extraction of the proton charge radius from the PRad data.

Acknowledgements

We thank Haiyan Gao, Claude Pruneau, and Weizhi Xiong for useful discussions. This work was supported by the U.S. Department of Energy grant DE-SC0007983 and by a Career Development Chair award from Wayne State University.

References

- [1] C. Alexandrou, K. Hadjiyiannakou, G. Koutsou, K. Ottnad and M. Petschlies, [arXiv:2002.06984 [hep-lat]].
- [2] R. Pohl *et al.*, Nature **466**, 213 (2010).
- [3] A. Antognini *et al.*, Science **339**, 417 (2013).
- [4] R. Gilman *et al.* [MUSE Collaboration], arXiv:1709.09753 [physics.ins-det].
- [5] P. J. Mohr, B. N. Taylor and D. B. Newell, Rev. Mod. Phys. **80**, 633 (2008) [arXiv:0801.0028 [physics.atom-ph]].
- [6] G. Paz, eConf C1907293 (2019) [arXiv:1909.08108 [hep-ph]].
- [7] A. Beyer *et al.*, Science **358**, 79 (2017).
- [8] N. Bezginov *et al.*, Science **365**, 1007 (2019).
- [9] H. Fleurbaey *et al.*, Phys. Rev. Lett. **120**, 183001 (2018) [arXiv:1801.08816 [physics.atom-ph]].
- [10] See the talks at the 2018 MITP workshop “Precision Measurements and Fundamental Physics: The Proton Radius Puzzle and Beyond”
<https://indico.mitp.uni-mainz.de/event/132/timetable/#all>
- [11] M. Mihovilović *et al.*, Phys. Lett. B **771**, 194 (2017) [arXiv:1612.06707 [nucl-ex]].
- [12] W. Xiong *et al.*, Nature **575**, no. 7781, 147 (2019).
- [13] D. W. Higinbotham, A. A. Kabir, V. Lin, D. Meekins, B. Norum and B. Sawatzky, Phys. Rev. C **93**, 055207 (2016) [arXiv:1510.01293 [nucl-ex]].
- [14] K. Griffioen, C. Carlson and S. Maddox, Phys. Rev. C **93**, no. 6, 065207 (2016) [arXiv:1509.06676 [nucl-ex]].
- [15] M. Horbatsch, E. A. Hessels and A. Pineda, Phys. Rev. C **95**, 035203 (2017) [arXiv:1610.09760 [nucl-th]].

- [16] M. Horbatsch and E. A. Hessels, Phys. Rev. C **93**, 015204 (2016) [arXiv:1509.05644 [nucl-ex]].
- [17] J. M. Alarcón, D. W. Higinbotham, C. Weiss and Z. Ye, Phys. Rev. C **99**, 044303 (2019) [arXiv:1809.06373 [hep-ph]].
- [18] K. Nakamura *et al.* [Particle Data Group], J. Phys. G **37**, 075021 (2010).
- [19] R. J. Hill and G. Paz, Phys. Rev. D **82**, 113005 (2010) [arXiv:1008.4619 [hep-ph]].
- [20] G. Lee, J. R. Arrington and R. J. Hill, Phys. Rev. D **92**, no. 1, 013013 (2015) [arXiv:1505.01489 [hep-ph]].
- [21] https://wiki.jlab.org/pcrewiki/index.php/PRad_Results
- [22] F. J. Ernst, R. G. Sachs and K. C. Wali, Phys. Rev. **119**, 1105 (1960).
- [23] R. J. Hill, eConf C **060409**, 027 (2006) [hep-ph/0606023].
- [24] Z. Epstein, G. Paz and J. Roy, Phys. Rev. D **90**, no.7, 074027 (2014) [arXiv:1407.5683 [hep-ph]].
- [25] C. A. Pruneau, “Data Analysis Techniques for Physical Scientists,” (Cambridge University Press, Cambridge, 2017).
- [26] J. Bernauer *et al.* [A1], Phys. Rev. Lett. **105**, 242001 (2010) [arXiv:1007.5076 [nucl-ex]].
- [27] J. Bernauer *et al.* [A1], Phys. Rev. C **90**, no.1, 015206 (2014) [arXiv:1307.6227 [nucl-ex]].
- [28] M. Horbatsch, Phys. Lett. B **804**, 135373 (2020) [arXiv:1912.01735 [nucl-ex]].
- [29] J. Alarcón, D. Higinbotham and C. Weiss, [arXiv:2002.05167 [hep-ph]]
- [30] K. Borah, R. J. Hill, G. Lee and O. Tomalak, [arXiv:2003.13640 [hep-ph]].